



HAL
open science

Sub-pixel detection in hyperspectral imaging with elliptically contoured t-distributed background

Olivier Besson, François Vincent

► **To cite this version:**

Olivier Besson, François Vincent. Sub-pixel detection in hyperspectral imaging with elliptically contoured t-distributed background. *Signal Processing*, 2020, 175, pp.107662-107667. 10.1016/j.sigpro.2020.107662 . hal-02798974

HAL Id: hal-02798974

<https://hal.science/hal-02798974>

Submitted on 5 Jun 2020

HAL is a multi-disciplinary open access archive for the deposit and dissemination of scientific research documents, whether they are published or not. The documents may come from teaching and research institutions in France or abroad, or from public or private research centers.

L'archive ouverte pluridisciplinaire **HAL**, est destinée au dépôt et à la diffusion de documents scientifiques de niveau recherche, publiés ou non, émanant des établissements d'enseignement et de recherche français ou étrangers, des laboratoires publics ou privés.



Open Archive Toulouse Archive Ouverte (OATAO)

OATAO is an open access repository that collects the work of some Toulouse researchers and makes it freely available over the web where possible.

This is an author's version published in: <https://oatao.univ-toulouse.fr/26072>

Official URL : <https://doi.org/10.1016/j.sigpro.2020.107662>

To cite this version :

Besson, Olivier and Vincent, François Sub-pixel detection in hyperspectral imaging with elliptically contoured t-distributed background. (2020) Signal Processing, 175. 107662-107667. ISSN 0165-1684

Any correspondence concerning this service should be sent to the repository administrator:

tech-oatao@listes-diff.inp-toulouse.fr

Short communication

Sub-pixel detection in hyperspectral imaging with elliptically contoured t -distributed background

Olivier Besson^{a,*}, François Vincent^a

University of Toulouse, ISAE-SUPAERO, 10 Avenue Edouard Belin, 31055 Toulouse, France

A B S T R A C T

Detection of a target with known spectral signature when this target may occupy only a fraction of the pixel is an important issue in hyperspectral imaging. We recently derived the generalized likelihood ratio test (GLRT) for such sub-pixel targets, either for the so-called replacement model where the presence of a target induces a decrease of the background power, due to the sum of abundances equal to one, or for a mixed model which alleviates some of the limitations of the replacement model. In both cases, the background was assumed to be Gaussian distributed. The aim of this short communication is to extend these detectors to the broader class of elliptically contoured distributions, more precisely matrix-variate t -distributions with unknown mean and covariance matrix. We show that the generalized likelihood ratio tests in the t -distributed case coincide with their Gaussian counterparts, which confers the latter an increased generality for application. The performance as well as the robustness of these detectors are evaluated through numerical simulations.

Keywords:

Detection
Generalized likelihood ratio test
Hyperspectral imaging
Replacement model
Student distribution

1. Problem statement

Hyperspectral imaging has become an increasingly popular tool for remote sensing and scene information retrieval, whether for civil or military needs and in a large number of applications, including analysis of the spectral content of soils, vegetation or minerals, detection of man-made materials or vehicles, to name a few [1,2]. One of the challenges of hyperspectral imaging is to detect a target -whose spectral signature is assumed to be known- within a background whose statistical properties are not fully known [3–5]. Depending on the spatial resolution of hyperspectral sensors and the size of the target, the latter may occupy the totality or only a fraction of the pixel under test (PUT), in which case one speaks of sub-pixel targets. In the latter case, the target replaces part of the background in the PUT, leading to the so-called replacement model [6,7].

Whatever the case, full-pixel or sub-pixel targets, the problem can be formulated as a conventional composite hypothesis problem [3–9]: given a vector $\mathbf{y} \in \mathbb{R}^p$ -where p denotes the number of spectral bands used- which represents the reflectance in the PUT, is there a component along \mathbf{t} -the signature of interest (Sol)- in addition to the background? Since the background statistics depend on unknown parameters (for instance mean and covariance

matrix) a set of training samples $\mathbf{Z} \in \mathbb{R}^{p \times n}$, hopefully free of the Sol \mathbf{t} , is observed whose statistics are assumed to match those of the background in the PUT. These training samples are gathered in the vicinity of the PUT (local detection) or along the whole image (global detection).

Recently in [10] we addressed sub-pixel detection using the replacement model under a Gaussian background, and we derived the plain generalized likelihood ratio test (GLRT) by maximizing the joint distribution of (\mathbf{y}, \mathbf{Z}) with respect to all unknown parameters. Moreover, motivated by some limitations of the replacement model, especially the fact that the filling factor of a sub-pixel target may not be in practice as large as expected, we also derived the GLRT for a mixed model where presence of a target induces a partial replacement of the background [11]. These two detectors assume a Gaussian background. However, evidence of non-Gaussianity of hyperspectral data has been brought [12,13] and therefore it is of interest to extend detectors originally devised for Gaussian background to the broader class of elliptically contoured (EC) distributions [14,15]. The aim of this communication is thus to extend our recent GLRTs from the Gaussian case to the matrix variate t -distributed case. We will show that the GLRTs coincide with their Gaussian counterparts. The paper is organized as follows. In Section 2, we consider each of the three models and derive the corresponding GLRTs. The latter are evaluated in Section 3 on simulated data but where the target spectral signature, the mean and covariance matrix of the background are obtained from real hyperspectral images.

* Corresponding author.

E-mail addresses: olivier.besson@isae-supaero.fr (O. Besson), francois.vincent@isae-supaero.fr (F. Vincent).

2. GLRT for matrix variate t -distributed background

As stated before, let us assume that we wish to decide whether a given vector \mathbf{y} contains a signature of interest \mathbf{t} in the presence of disturbance \mathbf{z} whose mean value $\boldsymbol{\mu}$ and covariance matrix $\boldsymbol{\Sigma}$ are unknown, and let us assume that a set of training samples \mathbf{z}_i , $i = 1, \dots, n$ are available which share the same distribution as \mathbf{z} . These samples can be collected around the PUT or along the whole image. We simply assume here that $n > p$. Therefore, we would like to solve the following problem:

$$\begin{aligned} H_0 : \mathbf{y} = \mathbf{z}; \quad \mathbf{z}_i \stackrel{d}{=} \mathbf{z}, \quad i = 1, \dots, n \\ H_1 : \mathbf{y} = \alpha \mathbf{t} + \beta \mathbf{z}; \quad \mathbf{z}_i \stackrel{d}{=} \mathbf{z}, \quad i = 1, \dots, n \end{aligned} \quad (1)$$

where $\stackrel{d}{=}$ means ‘‘has the same distribution as’’. In (1), \mathbf{t} corresponds to the assumed spectral signature of the target and α denotes its unknown amplitude. When $\beta = 1$ one obtains the conventional additive model. When $\beta = 1 - \alpha$ the replacement model is recovered, and the mixed model corresponds to an arbitrary β .

In order to derive the GLRT, we need to specify the joint distribution of \mathbf{y} and \mathbf{Z} where $\mathbf{Z} = [\mathbf{z}_1 \quad \mathbf{z}_2 \quad \dots \quad \mathbf{z}_n]$. As said in the introduction, we assume that $[\mathbf{y} \quad \mathbf{Z}]$ follows a matrix-variate t -distribution with ν degrees of freedom so that we need to solve the following composite hypothesis testing problem:

$$\begin{aligned} H_0 : [\mathbf{y} \quad \mathbf{Z}] \stackrel{d}{=} \mathcal{T}_{p, n+1}(\nu, \mathbf{M}_0, (\nu - 2)\boldsymbol{\Sigma}, \mathbf{I}_{n+1}) \\ H_1 : [\mathbf{y} \quad \mathbf{Z}] \stackrel{d}{=} \mathcal{T}_{p, n+1}\left(\nu, \mathbf{M}_1, (\nu - 2)\boldsymbol{\Sigma}, \begin{pmatrix} \beta^2 & \mathbf{0}^T \\ \mathbf{0} & \mathbf{I}_n \end{pmatrix}\right) \end{aligned} \quad (2)$$

where $\mathbf{M}_0 = [\boldsymbol{\mu} \quad \boldsymbol{\mu} \mathbf{1}_n^T]$, $\mathbf{M}_1 = [\alpha \mathbf{t} + \beta \boldsymbol{\mu} \quad \boldsymbol{\mu} \mathbf{1}_n^T]$, $\mathbf{1}_n$ is a $n \times 1$ vector with all elements equal to one, $\boldsymbol{\mu}$ stands for the mean value of the background while $\boldsymbol{\Sigma}$ denotes its covariance matrix. In (2), $\mathcal{T}(\cdot)$ stands for the matrix variate t -distribution [16,17] so that the probability density function (p.d.f.) of the observations under each hypothesis is given by

$$\begin{aligned} p_0(\mathbf{y}, \mathbf{Z}) &= C |\boldsymbol{\Sigma}|^{-\frac{n+1}{2}} \left| \mathbf{I}_p + \frac{\boldsymbol{\Sigma}^{-1}}{\nu - 2} [\mathbf{y} - \boldsymbol{\mu} \quad \mathbf{Z} - \boldsymbol{\mu} \mathbf{1}_n^T] \right. \\ &\quad \times \left. [\mathbf{y} - \boldsymbol{\mu} \quad \mathbf{Z} - \boldsymbol{\mu} \mathbf{1}_n^T]^T \right|^{-\frac{\nu+n+p}{2}} \\ p_1(\mathbf{y}, \mathbf{Z}) &= C \beta^{-p} |\boldsymbol{\Sigma}|^{-\frac{n+1}{2}} \left| \mathbf{I}_p + \frac{\boldsymbol{\Sigma}^{-1}}{\nu - 2} [\tilde{\mathbf{y}} - \boldsymbol{\mu} \quad \mathbf{Z} - \boldsymbol{\mu} \mathbf{1}_n^T] \right. \\ &\quad \times \left. [\tilde{\mathbf{y}} - \boldsymbol{\mu} \quad \mathbf{Z} - \boldsymbol{\mu} \mathbf{1}_n^T]^T \right|^{-\frac{\nu+n+p}{2}} \end{aligned} \quad (3)$$

with $\tilde{\mathbf{y}} = \beta^{-1}(\mathbf{y} - \alpha \mathbf{t})$ and $C = \frac{\Gamma_p((\nu+n+p)/2)}{\pi^{p(n+1)/2} \Gamma_p((\nu+p-1)/2)}$. It should be observed that the columns of $[\mathbf{y} \quad \mathbf{Z}]$ are only uncorrelated but not independent, as $p(\mathbf{y}, \mathbf{z}_1, \dots, \mathbf{z}_n)$ cannot be factored as $p(\mathbf{y}) \prod_{i=1}^n p(\mathbf{z}_i)$.

We now derive the GLRT for the problem in (2). Let us start by considering the following function $f(\boldsymbol{\Sigma})$ where \mathbf{S} is some positive definite matrix:

$$\begin{aligned} f(\boldsymbol{\Sigma}) &= |\boldsymbol{\Sigma}|^{-\frac{n+1}{2}} \left| \mathbf{I}_p + (\nu - 2)^{-1} \boldsymbol{\Sigma}^{-1} \mathbf{S} \right|^{-\frac{\nu+n+p}{2}} \\ &= |\boldsymbol{\Sigma}|^{\frac{\nu+p-1}{2}} \left| \boldsymbol{\Sigma} + (\nu - 2)^{-1} \mathbf{S} \right|^{-\frac{\nu+n+p}{2}} \end{aligned} \quad (4)$$

Differentiation of $\log f(\boldsymbol{\Sigma})$ yields

$$\frac{\partial \log f(\boldsymbol{\Sigma})}{\partial \boldsymbol{\Sigma}} = \frac{\nu + p - 1}{2} \boldsymbol{\Sigma}^{-1} - \frac{\nu + n + p}{2} (\boldsymbol{\Sigma} + (\nu - 2)^{-1} \mathbf{S})^{-1}. \quad (5)$$

Setting this derivative of to zero, we can see that $f(\boldsymbol{\Sigma})$ achieves its maximum at

$$\boldsymbol{\Sigma}_* = \frac{(\nu + p - 1)\mathbf{S}}{(\nu - 2)(n + 1)} = \gamma \mathbf{S} \quad (6)$$

It follows that

$$\begin{aligned} \max_{\boldsymbol{\Sigma}} p_0(\mathbf{y}, \mathbf{Z}) &= C' \left| [\mathbf{y} - \boldsymbol{\mu} \quad \mathbf{Z} - \boldsymbol{\mu} \mathbf{1}_n^T] \begin{bmatrix} (\mathbf{y} - \boldsymbol{\mu})^T \\ (\mathbf{Z} - \boldsymbol{\mu} \mathbf{1}_n^T)^T \end{bmatrix} \right|^{-\frac{n+1}{2}} \\ \max_{\boldsymbol{\Sigma}} p_1(\mathbf{y}, \mathbf{Z}) &= C' \beta^{-p} \left| [\tilde{\mathbf{y}} - \boldsymbol{\mu} \quad \mathbf{Z} - \boldsymbol{\mu} \mathbf{1}_n^T] \begin{bmatrix} (\tilde{\mathbf{y}} - \boldsymbol{\mu})^T \\ (\mathbf{Z} - \boldsymbol{\mu} \mathbf{1}_n^T)^T \end{bmatrix} \right|^{-\frac{n+1}{2}} \end{aligned} \quad (7)$$

with $C' = C \gamma^{-p(n+1)/2} [1 + (\nu - 2)^{-1} \gamma^{-1}]^{-p(\nu+n+p)/2}$. Since C' is the same under H_0 and H_1 it will cancel out in the GLR and therefore the GLR does not depend on ν . This means that ν does not need to be known since its estimation is not actually required to obtain the GLR.

Now, for any vector \mathbf{x} ,

$$\begin{aligned} \mathbf{M}(\boldsymbol{\mu}) &= [\mathbf{x} - \boldsymbol{\mu} \quad \mathbf{Z} - \boldsymbol{\mu} \mathbf{1}_n^T] [\mathbf{x} - \boldsymbol{\mu} \quad \mathbf{Z} - \boldsymbol{\mu} \mathbf{1}_n^T]^T \\ &= (\mathbf{x} - \boldsymbol{\mu})(\mathbf{x} - \boldsymbol{\mu})^T + (\mathbf{Z} - \boldsymbol{\mu} \mathbf{1}_n^T)(\mathbf{Z} - \boldsymbol{\mu} \mathbf{1}_n^T)^T \\ &= \mathbf{x} \mathbf{x}^T - \boldsymbol{\mu} \mathbf{x}^T - \mathbf{x} \boldsymbol{\mu}^T + \boldsymbol{\mu} \boldsymbol{\mu}^T \\ &\quad + \mathbf{Z} \mathbf{Z}^T - \boldsymbol{\mu} \mathbf{1}_n^T \mathbf{Z}^T - \mathbf{Z} \mathbf{1}_n \boldsymbol{\mu}^T + n \boldsymbol{\mu} \boldsymbol{\mu}^T \\ &= (n + 1) \boldsymbol{\mu} \boldsymbol{\mu}^T - \boldsymbol{\mu} (\mathbf{x} + \mathbf{Z} \mathbf{1}_n)^T - (\mathbf{x} + \mathbf{Z} \mathbf{1}_n) \boldsymbol{\mu}^T \\ &\quad + \mathbf{x} \mathbf{x}^T + \mathbf{Z} \mathbf{Z}^T \\ &= (n + 1) \left[\boldsymbol{\mu} - \frac{\mathbf{x} + \mathbf{Z} \mathbf{1}_n}{n + 1} \right] \left[\boldsymbol{\mu} - \frac{\mathbf{x} + \mathbf{Z} \mathbf{1}_n}{n + 1} \right]^T \\ &\quad + \mathbf{x} \mathbf{x}^T + \mathbf{Z} \mathbf{Z}^T - \frac{(\mathbf{x} + \mathbf{Z} \mathbf{1}_n)(\mathbf{x} + \mathbf{Z} \mathbf{1}_n)^T}{n + 1} \\ &= (n + 1) \left[\boldsymbol{\mu} - \frac{\mathbf{x} + \mathbf{Z} \mathbf{1}_n}{n + 1} \right] \left[\boldsymbol{\mu} - \frac{\mathbf{x} + \mathbf{Z} \mathbf{1}_n}{n + 1} \right]^T \\ &\quad + [\mathbf{x} \quad \mathbf{Z}] \left(\mathbf{I}_{n+1} - \frac{\mathbf{1}_{n+1} \mathbf{1}_{n+1}^T}{n + 1} \right) [\mathbf{x} \quad \mathbf{Z}]^T \end{aligned} \quad (8)$$

Consequently,

$$\min_{\boldsymbol{\mu}} |\mathbf{M}(\boldsymbol{\mu})| = \left| [\mathbf{x} \quad \mathbf{Z}] \mathbf{P}_{n+1}^\perp [\mathbf{x} \quad \mathbf{Z}]^T \right| \quad (9)$$

with \mathbf{P}_{n+1}^\perp the orthogonal projector on the null space of $\mathbf{1}_{n+1}$. Hence, we arrive at

$$\begin{aligned} \max_{\boldsymbol{\mu}, \boldsymbol{\Sigma}} p_0(\mathbf{y}, \mathbf{Z}) &= C' \left| [\mathbf{y} \quad \mathbf{Z}] \mathbf{P}_{n+1}^\perp [\mathbf{y} \quad \mathbf{Z}]^T \right|^{-\frac{n+1}{2}} \\ \max_{\boldsymbol{\mu}, \boldsymbol{\Sigma}} p_1(\mathbf{y}, \mathbf{Z}) &= C' \beta^{-p} \left| [\tilde{\mathbf{y}} \quad \mathbf{Z}] \mathbf{P}_{n+1}^\perp [\tilde{\mathbf{y}} \quad \mathbf{Z}]^T \right|^{-\frac{n+1}{2}} \end{aligned} \quad (10)$$

Next, for any vector \mathbf{x} and matrix \mathbf{Q} (not necessarily \mathbf{P}_{n+1}^\perp),

$$\begin{aligned} [\mathbf{x} \quad \mathbf{Z}] \mathbf{Q} [\mathbf{x} \quad \mathbf{Z}]^T &= [\mathbf{x} \quad \mathbf{Z}] \begin{bmatrix} \mathbf{Q}_{11} & \mathbf{Q}_{12} \\ \mathbf{Q}_{21} & \mathbf{Q}_{22} \end{bmatrix} [\mathbf{x} \quad \mathbf{Z}]^T \\ &= \mathbf{Q}_{11} \mathbf{x} \mathbf{x}^T + \mathbf{Z} \mathbf{Q}_{21} \mathbf{x}^T + \mathbf{x} \mathbf{Q}_{12} \mathbf{Z}^T + \mathbf{Z} \mathbf{Q}_{22} \mathbf{Z}^T \\ &= \mathbf{Q}_{11} [\mathbf{x} + \mathbf{Q}_{11}^{-1} \mathbf{Z} \mathbf{Q}_{21}] [\mathbf{x} + \mathbf{Q}_{11}^{-1} \mathbf{Z} \mathbf{Q}_{21}]^T \\ &\quad + \mathbf{Z} \mathbf{Q}_{2,1} \mathbf{Z}^T \end{aligned} \quad (11)$$

where $\mathbf{Q}_{2,1} = \mathbf{Q}_{22} - \mathbf{Q}_{21} \mathbf{Q}_{11}^{-1} \mathbf{Q}_{12}$. Therefore,

$$\begin{aligned} \left| [\mathbf{x} \quad \mathbf{Z}] \mathbf{Q} [\mathbf{x} \quad \mathbf{Z}]^T \right| &= \left| \mathbf{Z} \mathbf{Q}_{2,1} \mathbf{Z}^T \right| \times \\ \left[1 + \mathbf{Q}_{11} (\mathbf{x} + \mathbf{Q}_{11}^{-1} \mathbf{Z} \mathbf{Q}_{21})^T (\mathbf{Z} \mathbf{Q}_{2,1} \mathbf{Z}^T)^{-1} (\mathbf{x} + \mathbf{Q}_{11}^{-1} \mathbf{Z} \mathbf{Q}_{21}) \right] \end{aligned} \quad (12)$$

Coming back to the case $\mathbf{Q} = \mathbf{P}_{n+1}^\perp = \mathbf{I}_{n+1} - (n + 1)^{-1} \mathbf{1}_{n+1} \mathbf{1}_{n+1}^T$, we have

$$\mathbf{Q} = \begin{pmatrix} 1 & \mathbf{0}^T \\ \mathbf{0} & \mathbf{I}_n \end{pmatrix} - (n + 1)^{-1} \begin{pmatrix} 1 & \mathbf{1}_n^T \\ \mathbf{1}_n & \mathbf{1}_n \mathbf{1}_n^T \end{pmatrix} \quad (13)$$

so that

$$\begin{aligned}
Q_{11} &= 1 - (n+1)^{-1} = n(n+1)^{-1} \\
Q_{21} &= -(n+1)^{-1} \mathbf{1}_n \\
Q_{22} &= \mathbf{I}_n - (n+1)^{-1} \mathbf{1}_n \mathbf{1}_n^T \\
Q_{2,1} &= \mathbf{I}_n - n^{-1} \mathbf{1}_n \mathbf{1}_n^T = \mathbf{P}_n^\perp
\end{aligned} \tag{14}$$

It follows that $Q_{11}^{-1} \mathbf{Z} Q_{21} = -n^{-1} \mathbf{Z} \mathbf{1}_n = -\bar{\mathbf{z}}$ and $\mathbf{Z} Q_{2,1} \mathbf{Z}^T = \mathbf{Z} \mathbf{P}_n^\perp \mathbf{Z}^T = \mathbf{Z} \mathbf{Z}^T - n \bar{\mathbf{z}} \bar{\mathbf{z}}^T = \mathbf{S}$. Hence, the GLR is given by

$$\begin{aligned}
\text{GLR} &= \frac{[1 + Q_{11} (\mathbf{y} - \bar{\mathbf{z}})^T \mathbf{S}^{-1} (\mathbf{y} - \bar{\mathbf{z}})]^{(n+1)/2}}{\min_{\alpha, \beta} \beta^p [1 + Q_{11} (\tilde{\mathbf{y}} - \bar{\mathbf{z}})^T \mathbf{S}^{-1} (\tilde{\mathbf{y}} - \bar{\mathbf{z}})]^{(n+1)/2}} \\
&= \frac{[1 + \frac{n}{n+1} (\mathbf{y} - \bar{\mathbf{z}})^T \mathbf{S}^{-1} (\mathbf{y} - \bar{\mathbf{z}})]^{(n+1)/2}}{\min_{\alpha, \beta} \beta^p [1 + \frac{n}{n+1} (\frac{\mathbf{y} - \alpha \mathbf{t}}{\beta} - \bar{\mathbf{z}})^T \mathbf{S}^{-1} (\frac{\mathbf{y} - \alpha \mathbf{t}}{\beta} - \bar{\mathbf{z}})]^{(n+1)/2}}
\end{aligned} \tag{15}$$

A few important observations can be made regarding this result. First, for all three models, the GLRs in (15) coincide with their Gaussian counterparts. For the additive model a proof is given in Appendix A. A more intuitive way to figure out this equivalence is to realize that the expression of the GLR in (15) does not depend on ν and that, letting ν grow to infinity, one should recover the GLR for Gaussian distributed data. As for the replacement and the mixed models, the expression in (15) is exactly that of the ACUTE and SPADE detectors of [10] and [11] respectively, where the GLRTs for the replacement model and the mixed model are derived under the Gaussian assumption. Therefore, the latter are still GLRTs for a much broader class of distributions than initially expected.

Let us also briefly comment on the implementation of the GLRT. For the additive model $\beta = 1$, and the minimization problem in (15) is a simple linear least-squares problem for which a closed-form solution can be obtained. This yields

$$\begin{aligned}
\text{GLR}_{\text{AM}}^{2/(n+1)} &= \frac{1 + \frac{n}{n+1} (\mathbf{y} - \bar{\mathbf{z}})^T \mathbf{S}^{-1} (\mathbf{y} - \bar{\mathbf{z}})}{\min_{\alpha} 1 + \frac{n}{n+1} (\mathbf{y} - \bar{\mathbf{z}} - \alpha \mathbf{t})^T \mathbf{S}^{-1} (\mathbf{y} - \bar{\mathbf{z}} - \alpha \mathbf{t})} \\
&= \frac{1 + \frac{n}{n+1} (\mathbf{y} - \bar{\mathbf{z}})^T \mathbf{S}^{-1} (\mathbf{y} - \bar{\mathbf{z}})}{1 + \frac{n}{n+1} (\mathbf{y} - \bar{\mathbf{z}})^T \mathbf{S}^{-1} (\mathbf{y} - \bar{\mathbf{z}}) - \frac{n}{n+1} \frac{[(\mathbf{y} - \bar{\mathbf{z}})^T \mathbf{S}^{-1} \mathbf{t}]^2}{\mathbf{t}^T \mathbf{S}^{-1} \mathbf{t}}} \\
&\equiv \frac{\frac{n}{n+1} [(\mathbf{y} - \bar{\mathbf{z}})^T \mathbf{S}^{-1} \mathbf{t}]^2}{[1 + \frac{n}{n+1} (\mathbf{y} - \bar{\mathbf{z}})^T \mathbf{S}^{-1} (\mathbf{y} - \bar{\mathbf{z}})] [\mathbf{t}^T \mathbf{S}^{-1} \mathbf{t}]}
\end{aligned} \tag{16}$$

The GLR in (16) generalizes Kelly's detector to the case of a non-centered Student distributed background. Note that (16) differs from Kelly's detector by the $\frac{n}{n+1}$ factor.

As for the replacement model, $\beta = 1 - \alpha$ and the minimization should be conducted with respect to α only, i.e.,

$$\text{GLR}_{\text{RM}} = \frac{[1 + \frac{n}{n+1} \|\mathbf{S}^{-1/2} (\mathbf{y} - \bar{\mathbf{z}})\|^2]^{(n+1)/2}}{\min_{\alpha} (1 - \alpha)^p [1 + \frac{n}{n+1} \frac{\|\mathbf{S}^{-1/2} (\mathbf{y} - \alpha \mathbf{t} - (1 - \alpha) \bar{\mathbf{z}})\|^2}{(1 - \alpha)^2}]^{(n+1)/2}} \tag{17}$$

As shown in [10], this simply amounts to finding the (unique) positive root of a 2nd-order polynomial. Finally, for the mixed model where β is arbitrary, one has a 2-D minimization problem. However, minimization over α can be done analytically, leaving only a minimization over β :

$$\text{GLR}_{\text{MM}} = \frac{[1 + \frac{n}{n+1} \|\mathbf{S}^{-1/2} (\mathbf{y} - \bar{\mathbf{z}})\|^2]^{(n+1)/2}}{\min_{\beta} \beta^p [1 + \frac{n}{n+1} \frac{\|\mathbf{P}_{\mathbf{S}^{-1/2} \mathbf{t}}^\perp \mathbf{S}^{-1/2} (\mathbf{y} - \beta \bar{\mathbf{z}})\|^2}{\beta^2}]^{(n+1)/2}} \tag{18}$$

Again the solution is obtained as the unique positive root of a second-order polynomial equation [11]. Therefore for both the replacement model and the mixed model, all unknown parameters can be obtained in closed-form.

3. Numerical simulations

In the present section, we will compare the detectors developed above. The additive model GLR_{AM} in (16) will be referred to as mKELLY in the sequel as it consists in a slight modification of Kelly's original GLRT [18]. The replacement model GLR_{RM} in

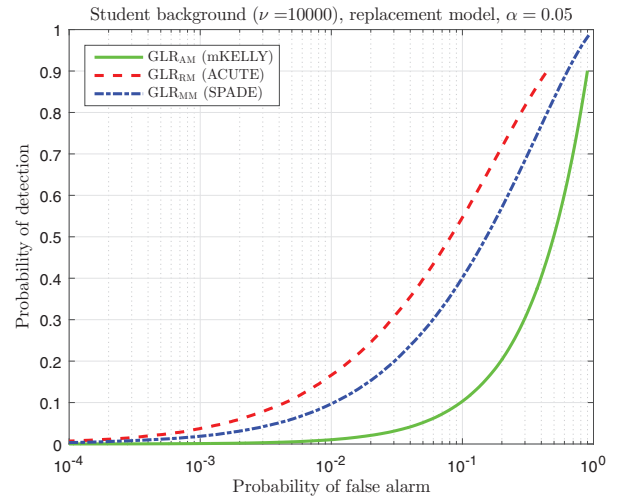
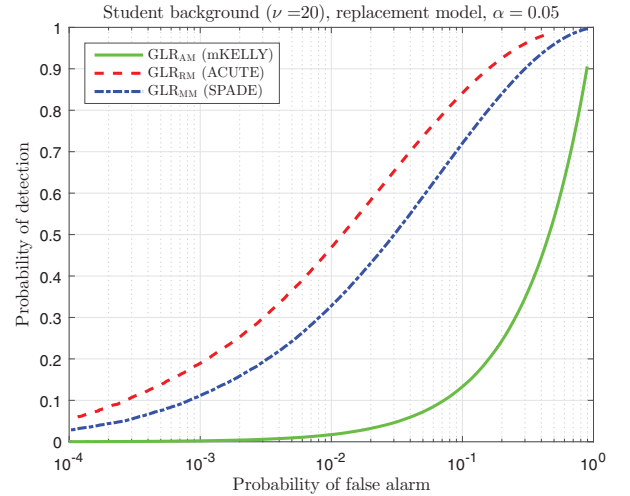
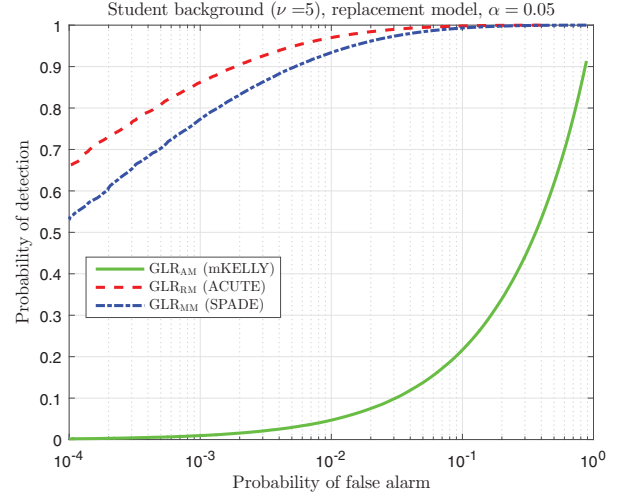


Fig. 1. ROC for the replacement model $\beta = (1 - \alpha)$.

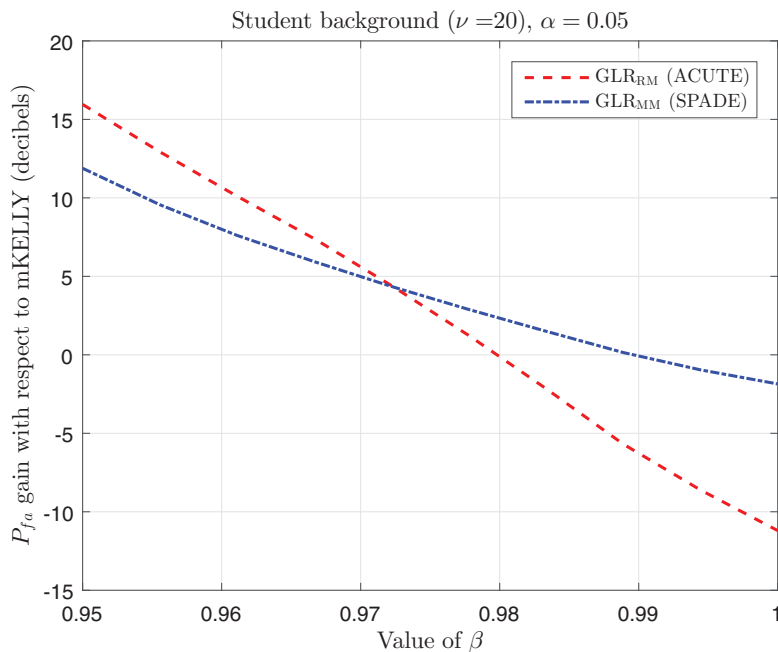


Fig. 2. P_{fa} gain versus β for $P_d = 0.5$.

(17) and the modified model GLR_{MM} in (18) will be referred as to ACUTE [10] and SPADE [11]. These last two detectors have already been assessed against real data drawn from the RIT [19] and Viareggio [20] experiments. Herein, we evaluate their performance as well as their robustness on simulated yet realistic data. More precisely we consider an image acquired in Viareggio (Italy) in May 2013 from an aircraft flying at 1200 meters. The original data is a $[450 \times 375]$ pixels map in the Visible Near InfraRed (VINR) band ($400 - 1000\text{nm}$) with a spatial resolution of about 0.6 meters. The scene is composed of parking lots, roads, buildings, sport fields and pine woods. Different kinds of vehicles as well as colored panels served as known targets. For each of these targets, a spectral signature obtained from ground spectroradiometer measurements is available. Herein, we consider \mathbf{t} to be the signature of the V5 target, $\boldsymbol{\mu}$ and $\boldsymbol{\Sigma}$ are respectively the sample mean and sample covariance matrix obtained from the whole Viareggio image. It has to be noticed that these raw radiance data have first been converted to reflectance measurements using an ELM method [21,22]. The number of spectral bands used is $p = 32$ and the number of training samples is $n = 60$. The background is simulated using a t distribution with ν degrees of freedom.

Fig. 1 plots the Receiver Operation Curve (ROC) obtained for the replacement model $[\beta = 1 - \alpha]$ with $\alpha = 0.05$, for different values of ν ranging from $\nu = 5$ (heavy-tailed distribution) to $\nu = 10,000$ (nearly Gaussian distributed background). As could be anticipated, ACUTE exhibits the best performance since it corresponds to the GLRT for the specific case $\beta = 1 - \alpha$. However, SPADE is shown to incur a small degradation compared to this optimal detector. On the contrary, mKELLY exhibits a significant performance loss, mostly because $\mathbb{E}\{\mathbf{z}\} \neq \mathbb{E}\{\mathbf{z}_k\}$, a fact that is not accounted for in the additive model, contrary to the other two detectors.

We now assess the robustness of ACUTE and SPADE. More precisely, we study their performance when β varies between $\beta = 1 - \alpha$ (replacement model) and $\beta = 1$ (additive model). In Fig. 2, we display the probability of false alarm (P_{fa}) gain of ACUTE and SPADE with respect to mKELLY, i.e., $10 \log_{10} \frac{P_{fa}(\text{GLR}_{\text{AM}})}{P_{fa}(\text{GLR}_{\text{RM/MM}})}$. This P_{fa} gain allows to measure the improvement (if positive) or the loss (when negative) of both ACUTE and SPADE with respect to mKELLY.

In this figure α is fixed to 0.05 and the probability of detection is $P_d = 0.5$. Fig. 2 confirms that ACUTE is slightly better than SPADE when the actual value of β is close to $1 - \alpha$. However, as soon as β departs from $1 - \alpha$ SPADE shows better performance than ACUTE. Moreover, SPADE performs better than mKELLY for most values of β unless β comes very close to 1, but in this case the loss of SPADE with respect to mKELLY is marginal. Therefore, SPADE provides the best robustness, with small performance loss compared to the optimal solution whatever the value of β .

4. Concluding remarks

In this communication, we considered the detection of a sub-pixel target in hyperspectral imaging when the background is no longer Gaussian but t -distributed. The GLRTs for a general mixed model, including the standard additive case and the replacement one, were derived, generalizing the Gaussian versions previously derived. For the three specific values of β considered in the literature, it was shown that the GLRTs remain the same and hence the detectors initially proposed under a Gaussian framework have more generality than expected. Moreover, they do not depend on the unknown degree of freedom of the t -distribution. Numerical simulations showed that SPADE provides a very good trade-off as it is always close to or better than Kelly and ACUTE which are optimal only for specific values of β .

Declaration of Competing Interest

The authors acknowledge that there is no conflict of interest regarding the paper entitled “Sub-pixel detection in hyperspectral imaging with elliptically contoured t -distributed back-ground”.

Appendix A. GLR for the additive model and Gaussian distributed background

In this appendix, we derive the GLRT for Gaussian distributed background and for the additive model. We thus consider the following detection problem

$$H_0 : [\mathbf{y} \quad \mathbf{Z}] \stackrel{d}{=} \mathcal{N}_{p,n+1}([\boldsymbol{\mu} \quad \boldsymbol{\mu} \mathbf{1}_n^T], \boldsymbol{\Sigma} \otimes \mathbf{I}_{n+1})$$

$$H_1 : [\mathbf{y} \quad \mathbf{Z}] \stackrel{d}{=} \mathcal{N}_{p,n+1}([\alpha \mathbf{t} + \boldsymbol{\mu} \quad \boldsymbol{\mu} \mathbf{1}_n^T], \boldsymbol{\Sigma} \otimes \mathbf{I}_{n+1}) \quad (\text{A.1})$$

The p.d.f. of (\mathbf{y}, \mathbf{Z}) is in this case

$$\begin{aligned} p_0(\mathbf{y}, \mathbf{Z}) &= (2\pi)^{-\frac{(n+1)p}{2}} |\boldsymbol{\Sigma}|^{-\frac{n+1}{2}} \\ &\times \text{etr} \left\{ -\frac{1}{2} \boldsymbol{\Sigma}^{-1} \begin{bmatrix} \mathbf{y} - \boldsymbol{\mu} & \mathbf{Z} - \boldsymbol{\mu} \mathbf{1}_n^T \end{bmatrix} \begin{bmatrix} (\mathbf{y} - \boldsymbol{\mu})^T \\ (\mathbf{Z} - \boldsymbol{\mu} \mathbf{1}_n^T)^T \end{bmatrix} \right\} \\ p_1(\mathbf{y}, \mathbf{Z}) &= (2\pi)^{-\frac{(n+1)p}{2}} |\boldsymbol{\Sigma}|^{-\frac{n+1}{2}} \\ &\times \text{etr} \left\{ -\frac{1}{2} \boldsymbol{\Sigma}^{-1} \begin{bmatrix} \mathbf{y} - \boldsymbol{\mu} & \mathbf{Z} - \boldsymbol{\mu} \mathbf{1}_n^T \end{bmatrix} \begin{bmatrix} (\mathbf{y} - \boldsymbol{\mu})^T \\ (\mathbf{Z} - \boldsymbol{\mu} \mathbf{1}_n^T)^T \end{bmatrix} \right\} \end{aligned} \quad (\text{A.2})$$

It is well-known that $|\boldsymbol{\Sigma}|^{-\frac{n+1}{2}} \text{etr}\{-\frac{1}{2} \boldsymbol{\Sigma}^{-1} \mathbf{S}\}$ achieves its maximum at $\boldsymbol{\Sigma}_* = (n+1)^{-1} \mathbf{S}$, and hence

$$\max_{\boldsymbol{\Sigma}} |\boldsymbol{\Sigma}|^{-\frac{n+1}{2}} \text{etr} \left\{ -\frac{1}{2} \boldsymbol{\Sigma}^{-1} \mathbf{S} \right\} = \left(\frac{e}{n+1} \right)^{-\frac{n+1}{2}} |\mathbf{S}|^{-\frac{n+1}{2}} \quad (\text{A.3})$$

It follows that $\max_{\boldsymbol{\Sigma}} p_0(\mathbf{y}, \mathbf{Z})$ and $\max_{\boldsymbol{\Sigma}} p_1(\mathbf{y}, \mathbf{Z})$ are proportional to (7) which holds for Student distributions. From there, everything follows and the GLRs for Student or Gaussian distributions are the same and are given by (15).

CRediT authorship contribution statement

Olivier Besson: Conceptualization, Methodology, Validation, Writing - original draft, Writing - review & editing, Visualization.
François Vincent: Conceptualization, Methodology, Software, Writing - original draft, Writing - review & editing.

References

- [1] M.T. Eismann, *Hyperspectral remote sensing*, SPIE, 2012.
- [2] D.G. Manolakis, R.B. Lockwood, T.W. Cooley, *Hyperspectral Imaging Remote Sensing*, Cambridge University Press, 2016.
- [3] D. Manolakis, G. Shaw, Detection algorithms for hyperspectral imaging applications, *IEEE Signal Process. Mag.* 19 (1) (2002) 29–43.
- [4] D. Manolakis, E. Truslow, M. Pieper, T. Cooley, M. Brueggeman, Detection algorithms in hyperspectral imaging systems: an overview of practical algorithms, *IEEE Signal Process. Mag.* 31 (1) (2014) 24–33.
- [5] N.M. Nasrabadi, Hyperspectral target detection: an overview of current and future challenges, *IEEE Signal Process. Mag.* 31 (1) (2014) 34–44.
- [6] D. Manolakis, G. Siracusa, G. Shaw, Hyperspectral subpixel detection using the linear mixing model, *IEEE Trans. Geosci. Remote Sens.* 39 (7) (2001) 1392–1409.
- [7] D. Manolakis, Hyperspectral signal models and implications to material detection algorithms, in: *Proceedings ICASSP*, volume 3, 2004, pp. 117–120.
- [8] R. DiPietro, D. Manolakis, R. Lockwood, T. Cooley, J. Jacobson, Performance evaluation of hyperspectral detection algorithms for sub-pixel objects, in: *Proceedings of SPIE - The International Society for Optical Engineering*, 2010.
- [9] J. Frontera-Pons, F. Pascal, J.-P. Ovarlez, Adaptive nonzero-mean Gaussian detection, *IEEE Trans. Geosci. Remote Sens.* 55 (2) (2017) 1117–1124.
- [10] F. Vincent, O. Besson, Generalized likelihood ratio test for subpixel target detection in hyperspectral imaging, *IEEE Trans. Geosci. Remote Sens.* 58 (6) (2020) 4479–4489, doi:10.1109/TGRS.2020.2965212.
- [11] F. Vincent, O. Besson, Generalized likelihood ratio test for modified replacement model in hyperspectral imaging detection, *Signal Process.* 174 (2020) paper 107643, doi:10.1016/j.sigpro.2020.107643.
- [12] D. Manolakis, D. Marden, G. Shaw, Hyperspectral image processing for automatic target detection applications, *Lincoln Lab. J.* 14 (1) (2003) 79–116.
- [13] S. Matteoli, M. Diani, G. Corsini, A tutorial overview of anomaly detection in hyperspectral images, *IEEE Aerosp. Electron. Syst. Mag.* 25 (7) (2010) 5–27.
- [14] T.W. Anderson, K.-T. Fang, *Theory and Applications of Elliptically Contoured and Related Distributions*, Technical Report, Department of Statistics, Stanford University, 1990.
- [15] F. Kai-Tai, Z. Yao-Ting, *Generalized Multivariate Analysis*, Springer Verlag, Berlin, 1990.
- [16] A.K. Gupta, D.K. Nagar, *Matrix Variate Distributions*, Chapman & Hall/CRC, Boca Raton, FL, 2000.
- [17] S. Kotz, S. Nadarajah, *Multivariate T Distributions and their Applications*, 2004.
- [18] E. Kelly, An adaptive detection algorithm, *IEEE Trans. Aerosp. Electron. Syst.* 22 (2) (1986) 115–127.
- [19] D. Snyder, J. Kerekes, I. Fairweather, R. Crabtree, J. Shive, S. Hager, Development of a web-based application to evaluate target finding algorithms, in: *Proceedings IGARSS 2008*, volume 2, Boston, MA, 2008.
- [20] N. Acito, S. Matteoli, A. Rossi, M. Diani, G. Corsini, Hyperspectral airborne “Viareggio 2013 trial” data collection for detection algorithm assessment, *IEEE J. Sel. Top. Appl. Earth Obs. Remote Sens.* 9 (6) (2016) 2356–2376.
- [21] G. Ferrier, Evaluation of apparent surface reflectance estimation methodologies, *Int. J. Remote Sens.* 16 (1995) 2291–2297.
- [22] G.M. Smith, E.J. Milton, The use of the empirical line method to calibrate remotely sensed data to reflectance, *Int. J. Remote Sens.* 20 (1999) 2653–2662.